Washington University School of Medicine

Digital Commons@Becker

4-1-2024

MYSM1 attenuates DNA damage signals triggered by physiologic and genotoxic DNA breaks

Brendan Mathias
Washington University School of Medicine in St. Louis

David O'Leary
Washington University School of Medicine in St. Louis

Nermina Saucier
Washington University School of Medicine in St. Louis

Faiz Ahmad
Washington University School of Medicine in St. Louis

Lynn S White
Washington University School of Medicine in St. Louis

See next page for additional authors

Recommended Citation

Authors

Brendan Mathias, David O'Leary, Nermina Saucier, Faiz Ahmad, Lynn S White, Le'Mark Russell, Marwan Shinawi, Matthew J Smith, Roshini S Abraham, Megan A Cooper, Maleewan Kitcharoensakkul, Abby M Green, and Jeffrey J Bednarski

MYSM1 attenuates DNA damage signals triggered by physiologic and genotoxic DNA breaks

Brendan Mathias, PhD,[a] David O'Leary, BS,[a] Nermina Saucier, MS,[a] Faiz Ahmad, PhD,[b] Lynn S. White, BS,[a] Le'Mark Russell, BS,[a] Marwan Shinawi, MD,[a] Matthew J. Smith, BGS,[c] Roshini S. Abraham, PhD,[d] Megan A. Cooper, MD, PhD,[a] Maleewan Kitcharoensakkul, MD,[a] Abby M. Green, MD,[a] and Jeffrey J. Bednarski, MD, PhD[a]

St Louis, Mo; Rochester, Minn; and Columbus, Ohio

Background: Patients with deleterious variants in *MYSM1* have an immune deficiency characterized by B-cell lymphopenia, hypogammaglobulinemia, and increased radiosensitivity. MYSM1 is a histone deubiquitinase with established activity in regulating gene expression. MYSM1 also localizes to sites of DNA injury but its function in cellular responses to DNA breaks has not been elucidated.
Objectives: This study sought to determine the activity of MYSM1 in regulating DNA damage responses (DDRs) to DNA double-stranded breaks (DSBs) generated during immunoglobulin receptor gene (*Ig*) recombination and by ionizing radiation.
Methods: MYSM1-deficient pre– and non–B cells were used to determine the role of MYSM1 in DSB generation, DSB repair, and termination of DDRs.
Results: Genetic testing in a newborn with abnormal screen for severe combined immune deficiency, T-cell lymphopenia, and near absence of B cells identified a novel splice variant in *MYSM1* that results in nearly absent protein expression. Radiosensitivity testing in patient's peripheral blood lymphocytes showed constitutive γH2AX, a marker of DNA damage, in B cells in the absence of irradiation, suggesting a role for MYSM1 in response to DSBs generated during *Ig* recombination. Suppression of MYSM1 in pre–B cells did not alter generation or repair of *Ig* DSBs. Rather, loss of MYSM1 resulted in persistent DNA damage foci and prolonged DDR signaling. Loss of MYSM1 also led to protracted DDRs in U2OS cells with irradiation induced DSBs.
Conclusions: MYSM1 regulates termination of DNA damage responses but does not function in DNA break generation and repair. (J Allergy Clin Immunol 2024;153:1113-24.)

Inborn errors of immunity provide unique opportunities to investigate the role of identified genes in development and function of the immune system. In this regard, variants in *MYSM1* (Myb-like SWIRM and MPN domains 1) have been identified in patients with immune deficiency characterized by B-cell lymphopenia, hypogammaglobulinemia, defective hematopoiesis, and increased sensitivity to genotoxic agents.[1-5] Patients may also have reduced T cells, short stature, developmental delay, and skeletal abnormalities; although occurrence of these abnormalities is variable. Mysm1-deficient mice have lymphopenia and bone marrow failure similar to human disease.[6-11] Cell type–specific MYSM1 loss in early B cells blocks development at the pro– and pre–B cell stages.[7,9] In contrast, *Mysm1* deletion in mature B cells does not alter numbers or function.[7] Thus, MYSM1 is critical for early B-cell development.

MYSM1 is a histone H2A deubiquitinase (DUB) that was identified as a transcriptional regulator.[12-14] Monoubiquitination of H2A on lysine 119 (H2AK119Ub) represses transcription, and MYSM1 catalyzes removal of this ubiquitin moiety to initiate gene expression.[11-14] In early B cells, MYSM1 promotes expression of *Ebf1*, a critical transcriptional regulator of B-cell differentiation.[9,15-18] However, MYSM1 deficiency results in increased markers of DNA damage and increased sensitivity to genotoxic stress, which are not seen with loss of *Ebf1*.[2,10] Therefore, immune defects in MYSM1 deficiency are not explained solely by dysregulated *Ebf1*.

MYSM1-deficient lymphocytes have higher baseline (no exposure to genotoxins) levels of phosphorylated histone H2AX (γH2AX), a marker of DNA damage, as well as increased p53 and cell death after irradiation.[2,10] Deletion of p53 rescues B-cell populations in *MYSM1*-deficient mice.[19] These findings suggest that activation of cell death downstream of DNA damage may contribute to the lymphopenia observed with MYSM1 deficiency. MYSM1 has been shown to localize to DNA double-stranded breaks (DSBs) and to interact with ubiquitinated H2A at irradiation-induced DNA damage, but little is known about MYSM1 activity in a DNA damage response (DDR).[20,21] The potential impact of MYSM1 on DDR and contribution of this activity to the observed immune deficiency have not been explored.

Developing B cells must induce DSBs at immunoglobulin receptor gene (*Ig*) loci and resolve them in a timely fashion to survive and mature.[22-24] This process occurs in pro– and pre–B cells, the developmental stages impacted by loss of *Mysm1*.[7,9] *Ig* gene

recombination occurs through generation of DSBs by the RAG endonuclease (composed of RAG1 and RAG2) in the G_1 phase of the cell cycle.[23-25] RAG-induced DSBs are repaired by nonhomologous end joining to ensure proper gene assembly and ongoing lymphocyte development.[23,24] A highly conserved signaling network coordinates cellular responses to DSBs.[22-24,26-28] The primary signaling protein activated by DSBs in G_1-arrested cells is the ATM kinase, which orchestrates chromatin modifications at the site of DNA injury, including phosphorylation of histone H2AX and ubiquitination of H2A.[26-30] In response to DSBs, H2A is ubiquitinated on lysines 13 and 15 (abbreviated as H2AK15Ub) by the ubiquitin ligases RNF8 and RNF168.[29-33] H2AK15Ub serves as a binding site for 53BP1 (protein product of *TP53BP1*), which in turn recruits numerous proteins that coordinate DSB repair and activation of DDR.[31-37] Following DSB resolution, these DDR complexes (or foci) dissipate to terminate DDR. If DSBs are not repaired, DDR foci persist and promote activation of p53 and induction of apoptosis.[27,28] DDR foci are inactivated by DUBs, which remove ubiquitin chains from H2A and other targets.[21,29,30,38] In many cell types, USP51 resolves H2AK15Ub and terminates DDR.[39] Homologous proteins (USP3, USP37, USP44, and USP49) may have similar roles.[21,30,38-43] However, the DUBs that regulate DDR in developing B cells are not known. The marked B-cell lymphopenia and increased DNA damage signals observed in MYSM1 deficiency suggest that MYSM1 may regulate DDR during B-cell development.

We present a patient with a novel homozygous deleterious variant in *MYSM1* that results in nearly absent MYSM1 protein and increased DDR signaling in B cells even in the absence of exogenous DNA damaging agents. To investigate the function of MYSM1 in cellular responses to physiologic and genotoxic DNA injury, we suppressed MYSM1 in pre–B cells and non–B cells, respectively. We find that MYSM1 does not function in DSB generation or repair, but, rather, it regulates cessation of DDR signaling. Loss of MYSM1 results in prolonged DDR signals that may be detrimental to lymphocyte development and to cellular responses to genotoxins, more broadly. These findings provide new insights into B-cell lymphopoiesis and have important implications for clinical management of patients with *MYSM1* deficiency.

METHODS
Patient information

Written informed consent was obtained. Data was collected from the St Louis Children's Hospital Immunodeficiency Database and the medical record. Study (#201107235) was approved by the Washington University School of Medicine Institutional Review Board.

Clinical testing of DNA damage responses

DNA damage signaling in patient's PBMCs was assessed as previously described.[44] Briefly, PBMCs were rested overnight at 37°C in 5% CO_2 then reserved as unirradiated or subjected to 2 Gy irradiation in a cesium Cs 139 irradiator. At indicated times, samples were stained for surface markers and intracellular phosphoproteins, then quantified by flow cytometry. Anti-CD45, anti-CD3, and anti-CD19 were from Beckman Coulter (Indianapolis, Ind). Anti-NKp46 was from BioLegend (San Diego, Calif). Anti-pATM (Ser1981) and anti-gH2AX (Ser139) were from Thermo Fisher Scientific (Waltham, Mass). In the patient's sample, B-cell identity was confirmed by costaining with anti-HLA-DR (BioLegend). A minimum of 200 CD19$^+$ B-cell events in the patient's PMBCs were collected for analysis at each time point.

Genetic testing

Chromosome microarray was performed by Washington University Cytogenetics and Molecular Pathology Laboratory using Affymetrix CytoScan HD array. NextGen sequencing with concurrent deletion/duplication testing for panel of 26 genes associated with inborn errors of immunity and trio whole exome sequencing were performed by GeneDx (Stamford, Conn).

Cell lines. $Rag1^{-/-}$:*Bcl2* and $Art^{-/-}$:*Bcl2* Abelson-kinase transformed murine pre–B cells (abl pre–B cells) were previously described.[45,46] Wild-type abl pre–B cells were generated by transduction of bone marrow cells from mice expressing a *Bcl2* transgene with a retrovirus expressing the v-abl kinase as previously described.[47,48] Abl pre–B cells were cultured in Dulbecco modified Eagle medium with 10% FBS, 1% PenStrep, 1% sodium pyruvate, 1% nonessential amino acids, 1% L-glutamine, and 0.0004% β-mercaptoethanol. To induce cell cycle arrest and induction of RAG DSBs, abl pre–B cells were treated with 3 μmol/L imatinib (10^6 cells/mL) for indicated times.[45-49] U2OS cells were cultured in Dulbecco modified Eagle medium with GlutaMAX, 10% FBS, and 1% PenStrep. To generate DSBs, U2OS cells were exposed to 5 or 10 Gy irradiation using a cesium Cs 139 irradiator. All cell lines were verified by genotyping and confirmed to be free of *Mycoplasma*.

shRNA and cDNA expression. pMSCV-INV-GFP retroviral plasmid was a gift from Barry Sleckman.[47] For abl pre–B cells, short hairpin RNA (shRNA) targeting mouse *Mysm1* (5′-ACAGGAAAATTCTGGGTTAATA-3′) was cloned into the MSCV-hCD2-mir30 retroviral vector.[50] For U2OS cells, shRNA targeting human *MYSM1* (5′-ACCAGATGGCTCT-TATCGCTTA-3′) was cloned into lentiviral pFLRu-U6-YFP-Puro vector. cDNA encoding 5′ FLAG-tagged MYSM1 or MYSM1$^{\Delta E16}$ (*MYSM1* mRNA/cDNA with splicing of exon 15 to

exon 17 and absence of intervening exon 16) was cloned into the pOZ-IRES-hCD25 retroviral vector.[51] pEGFP-MYSM1 plasmid was a gift from Dr Stephen Jackson.[21] Retrovirus and lentivirus were produced in PlatE cells (Cell Biolabs, San Diego, Calif) and 293T cells, respectively, by transfection of the viral plasmids with Lipofectamine 2000 (Life Technologies, Carlsbad, Calif). For lentivirus, pCMV-VSV-G and pCMV-d8.2R were included in the transfection.[46,52] Viral supernatant was collected and pooled from 24 to 72 hours after transfection. Cells were transduced with unconcentrated virus in media with 5 μg/mL polybrene (Sigma-Aldrich, St Louis, Mo) as previously described.[50] Transduced cells were identified by flow cytometric assessment of hCD2, hCD25, or YFP. Abl pre–B cells expressing hCD2 were sorted using anti-hCD2 magnetic beads (Miltenyi Biotec, Bergisch Gladbach, Germany) according to the manufacturer's protocol. U2OS cells transduced with pFLRu vector were selected by culture with 1 μg/mL puromycin until all nontransduced cells died.

Western blot analyses. Western blots were done on whole cell lysates as previously described using anti-phospho-KAP1 antibody (Bethyl Laboratories, Montgomery, Tex), anti-PIM2 (Santa Cruz Biotechnology, Dallas, Tex), anti-FLAG (Sigma), anti-GAPDH (Cell Signaling Technology, Danvers, Mass), anti-phospho-CHK2 (Cell Signaling), and anti-EBF1 (Santa Cruz) antibodies.[51] Secondary horseradish peroxidase–conjugated anti-mouse IgG or anti-rabbit IgG were from Cell Signaling. Western blots were developed with Pierce ECL (Thermo Fisher Scientific) or ECL Prime (Cytiva, Marlborough, Mass) and quantitated using ImageJ (National Institutes of Health, Bethesda, Md).

RT-PCR. PCR over the break assay was performed as previously described.[48,49] Briefly, genomic DNA was isolated then digested with NEBNext dsDNA Fragmentase (New England Biolabs, Ipswich, Mass) for 10 minutes followed by PCR Cleanup (QIAGEN, Venlo, The Netherlands) as per manufacturer's instructions. mRNA was isolated using RNeasy (QIAGEN) and reverse transcribed using SuperScriptII (Life Technologies) according to manufacturers' protocol. RT-PCR was performed using Brilliant II SYBR Green (Agilent Technologies, Sigma-Aldrich) and acquired on QuantStudio 3 (Thermo Fisher Scientific). For PCR over the break analysis, values were normalized to PCR product spanning CD19, a control region of uncut genomic DNA. For mRNA, values were normalized to β-actin. Primer sequences are in Table E1 in this article's Online Repository (available at www.jacionline.org).

Immunofluorescence. Immunofluorescence was done as previously described.[49,53] U2OS cells were grown directly on coverslips. Abl pre–B cells were applied to coverslips at indicated times using Cell Tak (Corning, Corning, NY) at 37°C for 20 minutes. Abl pre–B cells were then extracted with 0.2% Triton in PBS for 10 minutes on ice. Both cell types were fixed with 3.2% paraformaldehyde. Cells were washed with IF Wash Buffer (PBS, 0.5% IGEPAL [Sigma], and 0.02% NaN₃), then incubated in IF Blocking Buffer (10% FBS in IF Wash Buffer) for 30 minutes at room temperature. Slides were stained with rabbit anti-53BP1 (1:500; Novus International, St Louis, Mo) in IF Blocking Buffer for 1 hour at room temperature. Slides were washed then stained with goat anti-rabbit IgG conjugated with Alexa Fluor 594 (1:1000; Invitrogen, Thermo Fisher Scientific) and Hoechst 33342 (Sigma-Aldrich) for 30 minutes at room temperature followed by mounting with Prolong Gold (Invitrogen). Microscopy was performed on an Olympus fluorescence microscope (BX-53; Olympus Corporation of the Americas, Center Valley, Pa) using an ApoN 60X/1.49 NA oil immersion lens or an UPlanS-Apo 100X/1.4 oil immersion lens and cellSens Dimension software (Olympus). Raw images were exported into Adobe Photoshop (Adobe, San Jose, Calif), and for any adjustment in image contrast or brightness, the levels function was applied. Foci were quantitated using ImageJ.

V(D)J reporter assay. Green fluorescent protein (GFP) was measured by flow cytometry prior to imatinib (0 hours, baseline) and at indicated times after imatinib treatment. Results were normalized to 0 hours.

Comet assay. Neutral comet assays were performed using CometAssay (Trevigen, Thermo Fisher Scientific) according to manufacturer's instructions. Cells were collected at indicated times and resuspended in PBS with LMAgarose (ratio of 1:10) at 3×10^5 cells/mL and then plated onto a comet slide and dried at 4°C in the dark. While light-protected, slides were immersed in cold lysis buffer solution for 1 hour then in cold Tris/Borate/EDTA for 30 minutes. Slides were electrophoresed at 25 V in cold Tris/Borate/EDTA for 30 minutes then washed with room temperature DNA precipitation solution (1 mol/L ammonium acetate in 95% ethanol) and fixed in 70% ethanol for 30 minutes. After fixation, slides were dried overnight and stained with SYBR gold (Invitrogen) for 30 minutes. Images were acquired by fluorescence microscope (DFC3000G; Leica, Wetzlar, Germany) and analyzed by OpenComet in ImageJ.

Statistical analysis

Statistical analyses were done by Student t-test using Prism (GraphPad Software, San Diego, Calif).

RESULTS
Novel MYSM1 variant in patient with B-cell aplasia

A 1-week-old healthy, Black male presented with abnormal newborn screen for severe combined immune deficiency. Detailed clinical history and evaluation are included in this article's Online Repository (available at www.jacionline.org). On physical exam, patient was small for gestational age, but no craniofacial or skeletal deformities were present. Laboratory evaluation identified nearly absent B cells, low T cells, and normal natural killer (NK) cells (Fig 1, *A*). Of total CD4⁺ T cells, 60% expressed naïve marker CD45RA. T-cell receptor excision circle testing was low at 1010 copies per 10⁶ CD3⁺ cells (normal >6794). T-cell proliferation to phytohemagglutinin was normal. No maternal T-cell engraftment was present. IgM was very low, and IgG was normal (Fig 1, *A*). Low B and T cells persisted through 2 months of age (Fig 1, *A*). He developed progressive normocytic anemia (hemoglobin 6.4 g/dL) with inappropriately low reticulocytosis (3%), resulting in red blood cell transfusion dependency. Bone marrow biopsy revealed multilineage hematopoiesis. Genetic testing by clinical whole exome sequencing identified a homozygous splice variant in *MYSM1* (c.1843-1G>A, IVS15-1 G>A variant) due to paternal uniparental disomy of chromosome 1. This variant is not observed in a general population.[54]

MYSM1 variant (c.1843-1G>A) results in aberrant mRNA splicing and absent protein

MYSM1 (c.1843-1G>A) variant alters the slice acceptor site prior to exon 16. Computational analysis predicted aberrant

A

	7 days old	2 mon old	Ref. (cells/ul)
T cells	847	491	2500-5500
CD4$^+$ T cells	416	181	1600-4000
CD8$^+$ T cells	370	207	560-1700
B cells	15	0	200-300
NK cells	554	123	170-1100
CD4$^+$CD45RA$^+$ T cells	60%	N.D.	n/a

At 7 days old:

IgG	IgM	IgA	IgE
661 mg/dl (nl = 251-1069)	2.3 mg/dl (nl = 20-149)	<7.0 mg/dl (nl = <7-90)	0.2 mg/dl (nl = 0.8-12)

B
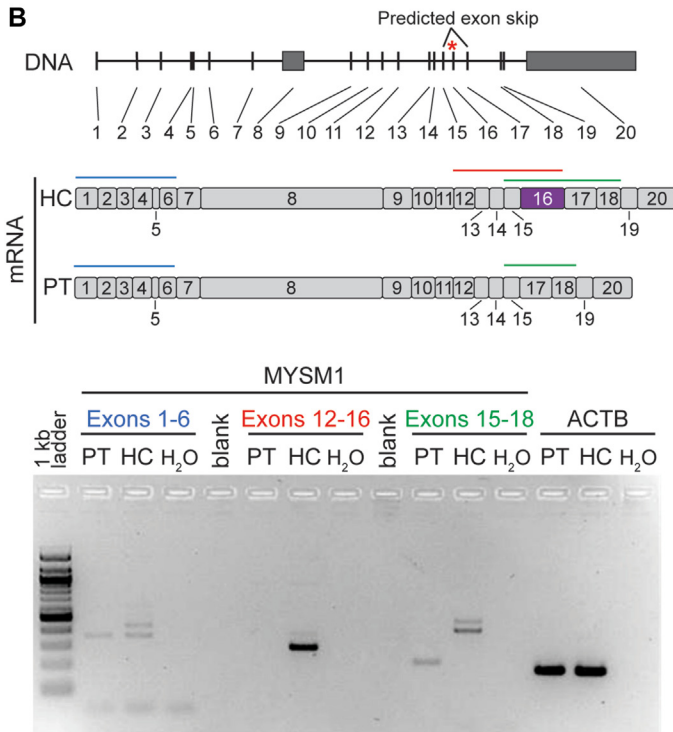
C
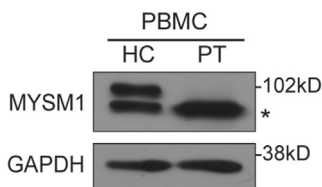
D
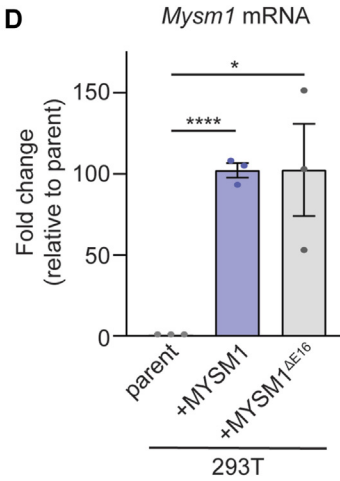
E
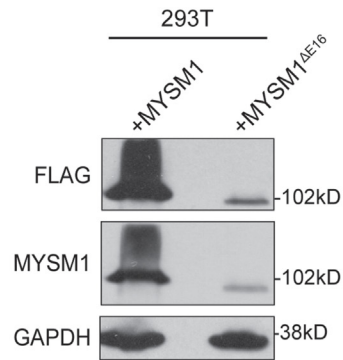
F
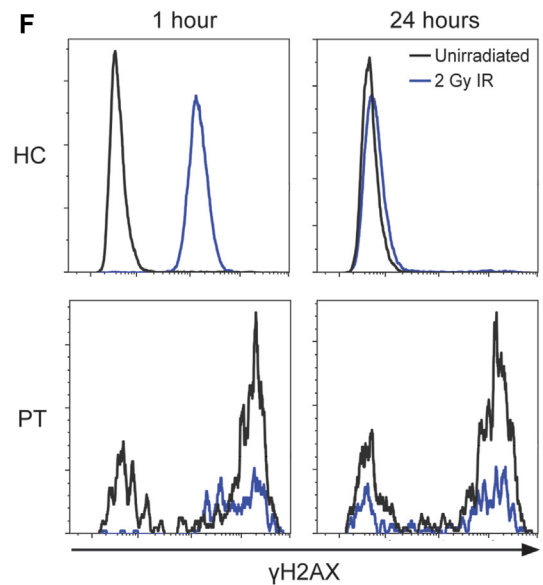
FIG 1. Novel MYSM1 splice variant in patient with B-cell lymphopenia, hypogammaglobulinemia, and increased DNA damage. **A,** Patient's lymphocyte numbers and immunoglobulin values. **B,** RT-PCR of mRNA isolated from PMBCs of patient (*PT*) and health control (*HC*). Schematic shows genomic *MYSM1* DNA with location of PT's c.1843-1G>A variant (*), mRNA for HC, and predicted mRNA for PT. Locations of PCR products for exons 1-6 (*blue*), exons 12-16 (*red*), and exon 15-18 (*green*) are indicated. Actin-B (*ACTB*) included as control. The 2 PCR products in exons 15-18 for HC are splice variants (see Fig E1). **C,** Western blot of MYSM1

slicing that skips exon 16, which encodes the DUB domain of MYSM1 (Fig 1, *B*). To determine functional consequences of this novel variant, we assessed *MYSM1* mRNA in patient PBMCs. RT-PCR analysis demonstrated an abnormal *MYSM1* mRNA transcript missing exon 16 (Fig 1, *B*). Sequencing confirmed patient expressed aberrant *MYSM1*$^{\Delta E16}$ mRNA (see Fig E1 in this article's Online Repository at www.jacionline.org).

The alternatively spliced transcript generated by the patient's *MYSM1*$^{\Delta E16}$ variant is in-frame with potential to encode for protein with a 63 amino acid deletion. Western blot analysis of patient PBMCs demonstrated loss of high molecular weight MYSM1 protein compared to healthy control PMBCs (Fig 1, *C*). Both control and patient PBMCs exhibited a lower molecular weight protein, which may represent a nonspecific band or a MYSM1 variant that overlaps with MYSM1$^{\Delta E16}$ expected size. To distinguish between these possibilities, we retrovirally expressed FLAG-tagged MYSM1 and MYSM1$^{\Delta E16}$ in 293T cells. *MYSM1* and *MYSM1*$^{\Delta E16}$ mRNA are equivalently expressed (Fig 1, *D*). In contrast, MYSM1$^{\Delta E16}$ protein was very low compared to wild-type MYSM1 (Fig 1, *E*). Collectively, these results demonstrate that *MYSM1* (c.1843-1G>A) variant results in abnormally spliced mRNA that encodes an unstable protein. Thus, clinically, our patient is effectively deficient in MYSM1 similar to reported patients with other *MYSM1* mutations.[1-5] Considering patient's phenotype, absence from large databases, and these functional studies, this *MYSM1* variant can be classified as pathogenic (PVS1, PS3, PM2, PP4) based on American College of Medical Genetics criteria.[55]

Increased DNA damage signaling in MYSM1-deficient B and T cells

Deficiency of MYSM1 in humans and mouse models has been shown to increase sensitivity to genotoxic stress.[2,3,21] To evaluate functional consequences of the novel MYSM1 variant identified in our patient, we assessed DDR in peripheral blood lymphocytes using an established clinical flow cytometry assay.[44] Phosphorylation of ATM (p-ATM) and H2AX (γH2AX) were measured in B, T, and NK cells (gating shown in Fig E2 in this article's Online Repository at www.jacionline.org) before and after exposure to 2 Gy ionizing radiation (IR). At baseline (unirradiated), 2 populations of patient B cells were present: a larger population with high constitutive levels of γH2AX, equivalent to post-IR levels, and a smaller subset with absent γH2AX similar to unirradiated healthy control B cells (Fig 1, *F*, black line). Notably, patient B cells did not have constitutive p-ATM in the absence of IR (see Fig E3, *A*, black line, in this article's Online Repository at www.jacionline.org). After IR, all healthy control B cells accumulated γH2AX and p-ATM at 1 hour, which resolved at 24 hours (Fig 1, *F* and Fig E3, *A*, blue lines). In contrast, all patient B cells expressed γH2AX at 1 hour after IR, but only a subset demonstrated p-ATM (Fig 1, *F* and Fig E3, *A*, blue lines). At 24 hours after IR, both γH2AX and p-ATM resolved to baseline with

persistence of the γH2AX-high B-cell subset. Testing to further characterize the developmental stage of the patient's B cells was not feasible as additional blood or bone marrow samples were not available.

Unlike B cells, patient T and NK cells had no evidence of constitutive γH2AX and had normal induction and resolution of γH2AX and p-ATM after IR, which is identical to healthy controls (see Fig E3, *B-E*). Cumulatively, these findings suggest that B cells are particularly sensitive to MYSM1 loss, including increased DNA damage signaling even in the absence of exogenous DNA damaging agents. These results may reflect aberrant responses to DSBs generated during *Ig* assembly in MYSM1-deficient B cells.

Loss of MYSM1 results in persistence of 53BP1 foci in response to DNA damage

Loss of MYSM1 results in increased DNA damage signaling in lymphocytes and nonlymphoid cells, but its function in cellular responses to DNA injury has not been characterized.[2,3,21] We investigated the role of MYSM1 in DDR to both programmed DSBs generated during *Ig* recombination and to genotoxic DSBs. To assess programmed DSBs, we used abl pre–B cells.[45-49] A human B-cell line for investigating *Ig* recombination is not available. Murine abl pre–B cells are a well-established system for studying molecular and biochemical characteristics of genetic defects in *Ig* recombination and DDRs identified in patients.[45-49,56,57] The Abl kinase promotes pre–B cell proliferation and suppresses *Ig* recombination. Inhibition of Abl kinase with imatinib induces G_1 cell cycle arrest, expression of the RAG endonuclease, and recombination of the immunoglobulin light chain gene (*Igl*) allele. *Igl* recombination proceeds through DSBs, which activate DDR signaling. Abl pre–B cells also expressed a *Bcl2* transgene to support survival after imatinib treatment, permitting quantitative evaluation of DDR.[45-49] We transduced wild-type abl pre–B cells with retrovirus expressing nontargeting shRNA (shNT) or shRNA targeting *Mysm1* (shMysm1) (Fig 2, *A*). Cells were subsequently treated with imatinib to induce *Igl* recombination and associated DDR signaling. At 48 hours after imatinib, ~40% of abl pre–B cells accumulated 1 to 2 53BP1 foci per cell (Fig 2, *B* and *C*). As expected, the percentage of cells with 53BP1 foci decreased by 72 hours after imatinib, which is consistent with DSB repair and resolution of DDR signaling. Suppression of MYSM1 did not affect generation of 53BP1 foci because abl pre–B cells expressing shMysm1 had equivalent 53BP1 foci compared to control cells expressing shNT at 48 hours after imatinib (Fig 2, *B* and *C*). In contrast, suppression of MYSM1 resulted in sustained increase in 53BP1 foci at 72 hours, indicative of delayed resolution of DNA damage signals (Fig 2, *B* and *C*). Notably, the persistence of 53BP1 foci with loss of MYSM1 is not due to alterations in EBF1 because abl pre–B cells expressing shMysm1 have no changes in EBF1 mRNA or

in PBMCs. GAPDH is loading control. Asterisk (*) indicates lower molecular weight protein that could represent splice variant or nonspecific band. **D** and **E**, 293T cells were transfected with vector expressing FLAG-tagged MYSM1 or MYSM1$^{\Delta E16}$. **D**, *MYSM1* mRNA. Parent is untransfected control. **E**, Western blot of FLAG and MYSM1. Blot is overexposed to visualize MYSM1$^{\Delta E16}$. GAPDH is loading control. **F**, Flow cytometry of γH2AX in B cells from HC and PT at indicated times after 2 Gy IR (*blue lines*). Unirradiated cells (*black lines*) included at each time as control. Data are mean $\pm$ SEM from 3 independent experiments **(D)** or are representative of 3 independent experiments **(E)**. *$P <$ .05, ****$P <$ .0001.
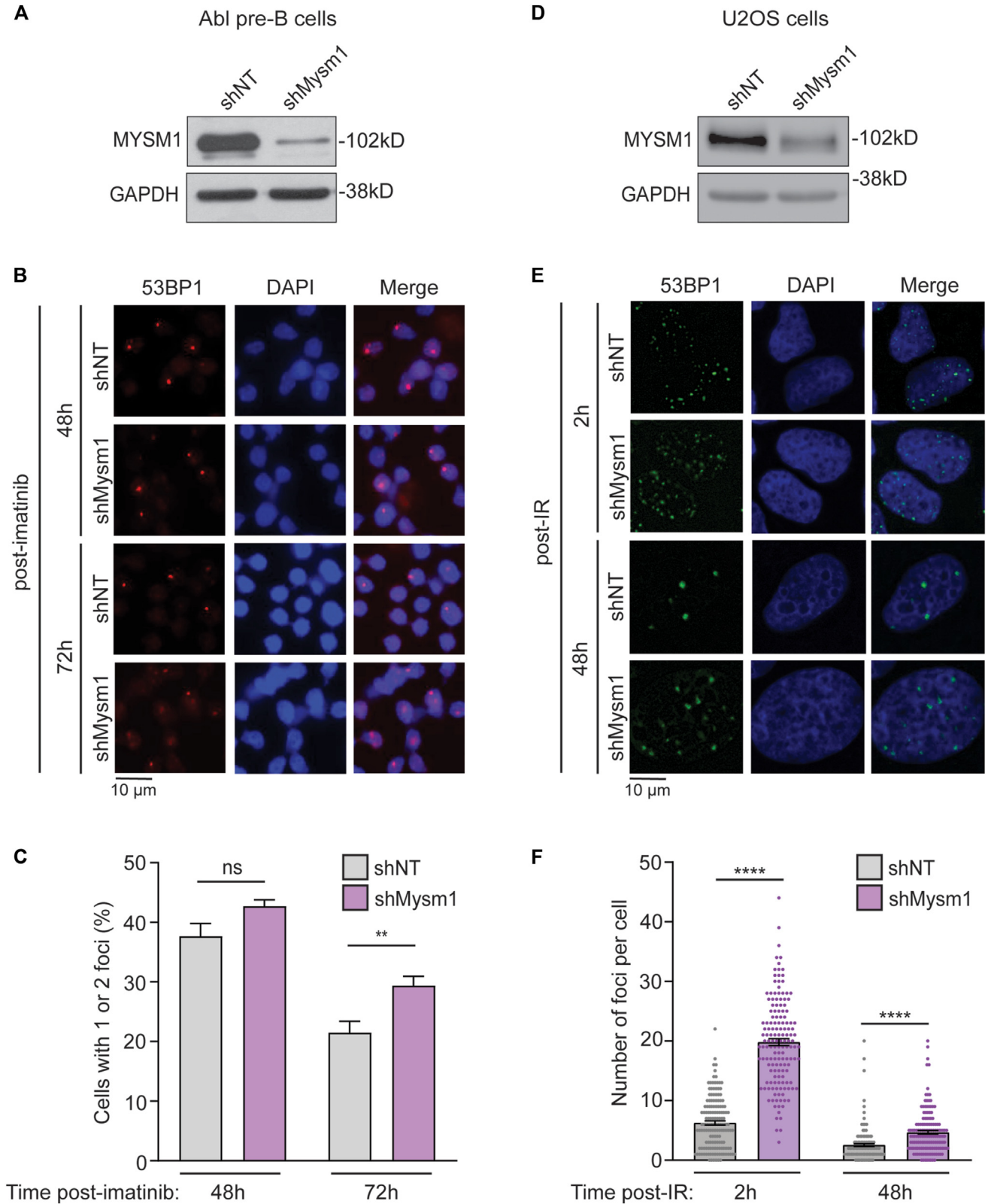
FIG 2. Loss of MYSM1 results in persistent 53BP1 foci. **A-C,** Wild-type abl pre–B cells were transduced with retrovirus expressing shNT or shMysm1. **A,** Western blot of MYSM1. GAPDH is loading control. **B,** Representative images of 53BP1 foci at 48 or 72 hours after treatment with imatinib to induce RAG DSBs. Bar = 10 μm. **C,** Quantitation of percentage of cells with 1-2 foci per cell in **B**. Data are mean ± SEM of 3 technical replicates and are representative of 3 independent experiments. **D-F,** U2OS cells were transduced with lentivirus expressing shNT or shMysm1. **D,** Western blot of MYSM1. GAPDH is loading control. **E,**

protein levels compared with control abl pre–B cells (see Fig E4 in this article's Online Repository at www.jacionline.org).

To determine whether MYSM1 also functions in DDR to genotoxic DSBs, U2OS cells were transduced with lentiviral vector expressing shNT or shMysm1 then exposed to IR (Fig 2, D). Both control cells (expressing shNT) and cells with loss of MYSM1 accumulated 53BP1 foci 2 hours after IR, which decreased by 48 hours. Compared with control cells, U2OS cells with MYSM1 depletion demonstrated significantly higher numbers of 53BP1 foci per cell at both 2 hours and 48 hours after IR (Fig 2, E and F). Thus, similar to findings in pre–B cells with RAG DSBs, loss of MYSM1 resulted in delayed resolution of 53BP1 foci after IR-induced DSBs. These results demonstrate that MYSM1 functions in responses to both physiologic and genotoxic DSBs across different cell types.

MYSM1 does not function in generation or repair of DSBs

Aberrant γH2AX and 53BP1 foci are typically interpreted as representing persist DSBs, but these signals can be indicative of abnormal DDR despite normal DSB resolution. To resolve whether MYSM1 functions in DSB generation/repair or DDR signaling, we measured DSBs during *Igl* recombination in abl pre–B cells and following IR in U2OS cells. We used Artemis-deficient ($Art^{-/-}$:*Bcl2*) abl pre–B cells, which generate persistent RAG DSBs at *Igl* because Artemis is required for DSB repair.[45,46,48] RAG-deficient ($Rag1^{-/-}$:*Bcl2*) abl pre--B cells, which do not generate DSBs, were included as a control.[45,46,48] Following imatinib treatment, $Art^{-/-}$:*Bcl2* abl pre–B cells generated RAG DSBs in ~50% of *Igl* loci (Fig 3, A). $Art^{-/-}$:*Bcl2* abl pre–B cells with suppression of MYSM1 (expressing shMysm1) had equivalent DSB generation as control cells (expressing shNT; Fig 3, A).

To further investigate MYSM1 function in DSB generation and repair, we transduced a repair-sufficient wild-type abl pre–B cell line with a recombination reporter containing an inverted GFP cDNA flanked by RAG target sequences (Fig 3, B). Expression of GFP requires both generation and repair of RAG DSBs.[47,57] Pre–B cells expressing shMysm1 had similar GFP expression as control cells (Fig 3, B). Together with the above results, these findings demonstrate that loss of MYSM1 in pre–B cells does not affect generation or repair of RAG-mediated DSBs.

We also investigated MYSM1 function in repair of IR-induced DSBs. U2OS cells were exposed to 10 Gy IR and DSBs were quantitated by comet assay. At 30 minutes after IR, U2OS cells had longer Olive moment, indicative of DSBs, that decreased by 48 hours, which is consistent with the expected kinetics of generation and repair of IR-induced DSBs (Fig 3, C). Suppression of MYSM1 did not alter Olive moment at any time, demonstrating that loss of MYSM1 does not affect generation or repair of genotoxic DSBs (Fig 3, C). In combination, the results in pre–B and U2OS cells indicate that MYSM1 regulates 53BP1 accumulation at DDR foci but does not function in DSB generation or repair.

Loss of MYSM1 results in persistent downstream DDR signaling

53BP1 coordinates signaling cascades downstream of DSBs and DDR activation.[34,36,37] MYSM1 deficiency results in persistent 53BP1 foci, which may stimulate sustained downstream DDR signals that, in turn, could impact cell fate. To determine whether DDR signaling persists with loss of MYSM1, we assessed DSB-regulated cellular programs in pre–B cells and U2OS cells.

In pre–B cells, RAG DSBs trigger canonical and noncanonical (developmental) DDR programs.[22,49] Canonical DDR includes p-KAP1, whereas noncanonical DDR includes upregulation of PIM2, a prosurvival factor that promotes continued B-cell maturation.[22,49,50,58] Suppression of MYSM1 in wild-type pre–B cells resulted in increased p-KAP1 and PIM2 compared to control pre–B cells (expressing shNT) at both 48 and 72 hours after RAG DSB generation (Fig 4, A and B). In control cells, PIM2 and p-KAP1 decrease at 72 hours compared to 48 hours, similar to the reduction in 53BP1 foci at this time, as expected with DSB repair and termination of DDR signaling (Figs 2, B and C and 4, A). Pre–B cells with MYSM1 depletion also had reduction in p-KAP1, PIM2, and 53BP1 foci from 48 to 72 hours, but the magnitude of decline is less than in control cells, which is consistent with persistence of DNA damage signaling (Figs 2, B and C and 4, A). Thus, in the absence of MYSM1, both downstream canonical and noncanonical DDRs are increased in magnitude and length of time in pre–B cells undergoing *Igl* recombination.

Similar to pre–B cells, knockdown of MYSM1 in U2OS cells resulted in increased p-KAP1 and p-CHK2, two key DDR signaling factors, after IR (Fig 4, C and D). Phosphorylation of both proteins was evident at 30 minutes after IR and then gradually declined. U2OS cells with loss of MYSM1 had higher p-KAP1 and p-CHK2 than control cells at each time. As DSBs are repaired, DDR signaling is normally attenuated as evidenced by decrease in p-KAP1 and p-CHK2 by 24 hours after IR (Fig 4, C). Notably, p-KAP1 and p-CHK2 declined in MYSM1-sufficient and -deficient cells, indicating that factors in addition to MYSM1 contribute to resolution of DDR signaling. Despite this redundancy, loss of MYSM1 resulted in higher magnitude of DDR signaling at later times after RAG- and IR-induced DSBs (Fig 4).

Increased MYSM1 accelerates DDR resolution

Persistence of DDR signals with reduction in MYSM1 suggests that cellular quantity of MYSM1 regulates kinetics of DDR resolution. To further investigate this, we transduced U2OS cells with a vector expressing GFP-tagged MYSM1, which substantially increased MYSM1 protein compared to endogenous levels in control cells transduced with empty vector (Fig 5, A). Compared with controls, cells with high MYSM1 had marked reduction in 53BP1 foci, p-KAP1, and p-CHK2 at 2 hours after IR (Fig 5, A-D). Indeed, many of the cells with high MYSM1 had almost no 53BP1 foci (Fig 5, C and D). Cells with high MYMS1 had significantly decreased p-KAP1 (Fig 5, A and B). Higher expression of MYSM1 also consistently reduced p-CHK2 (Fig 5, A and B); although, this did not reach statistical significance because the magnitude of reduction was more

Representative images of 53BP1 foci at 2 or 48 hours after exposure to 5 Gy IR. Bar = 10 μm. **F,** Quantitation of number of foci per cell in **E.** Data are mean ± SEM of 100 cells per condition and time. Results are representative of 3 independent experiments. ****P < .01; ****P < .0001.** *DAPI,* 4′-6-diamidino-2-phenylindole, dihydrochloride; *ns,* not significant.
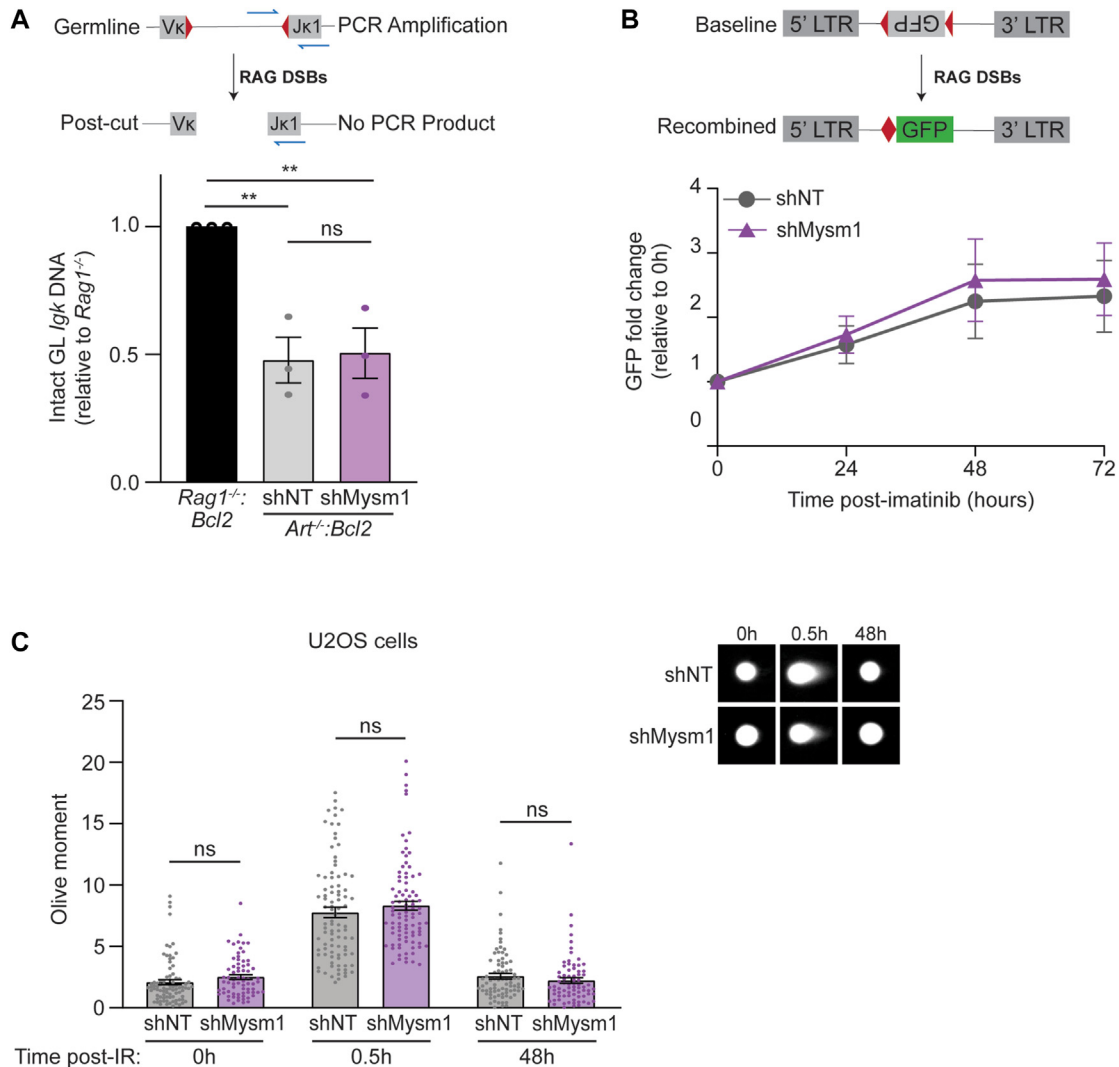
FIG 3. MYSM1 does not regulate DSB generation or repair. **A**, $Art^{-/-}$:Bcl2 abl pre–B cells expressing shNT or shMysm1 were treated with imatinib for 48 hours to induce RAG DSBs. DSBs were quantitated by quantitative PCR analysis of Igl ($Jk1$) genomic DNA. Schematic shows germline locus (GL), unrepaired DSB (post-cut), and primer location. Results are normalized to $Rag1^{-/-}$:Bcl2 abl pre–B cells, which do not generate DSBs and have only germline Igl. Loss of germline product is representative of DSB generation. **B**, Wild-type abl pre–B cells expressing shNT or shMysm1 (as in Fig 2, A) were transduced with a vector encoding a V(D)J reporter (schematic) then treated with imatinib to induce reporter recombination. GFP was measured by flow cytometry at indicated times and normalized to 0 hours. Data in **A** and **B** are mean ± SEM for 3 independent experiments. **C**, U2OS cells expressing shNT or shMysm1 (as in Fig 2, D) were exposed to 10 Gy IR. DSBs were quantitated by neutral comet assay at indicated times. Data are mean ± SEM for Olive moment of ≥45 cells per condition and time. Inset shows representative images of comet. Data are representative of 3 independent experiments. **P < .01.

variable (Fig 5, B). Importantly, increased expression of MYSM1 did not alter DSB generation (Fig 5, E). In combination with the MYSM1 depletion studies, these findings show that MYSM1 levels inversely correlate with DDR resolution.

DISCUSSION

Patients with MYSM1 deficiency have lymphopenia with disproportionate reduction in B cells and increased radiosensitivity.[1-5] Here we show that MYSM1 functions in termination of DDRs to resolve DDR foci and extinguish DDR signals. MYSM1 activity in DDR is conserved across both programmed and genotoxic DSBs generated at Igs during normal B-cell development and by exogenous DNA damaging agents, respectively. MYSM1 regulates resolution of 53BP1 retention at DSBs and downstream cellular responses but does not affect DSB generation or repair. Consequently, loss of MYSM1 results in continued DDR signaling without altering DSB number or persistence. MYSM1 activity in DDR may contribute to the immunopheno-type and clinical manifestations of patients with deleterious MYSM1 variants.

Mice with germline deletion of MYSM1 develop bone marrow failure and B-cell lymphopenia similar to MYSM1-deficiency in patients.[6-11] Cell type–specific deletion of MYSM1 in early
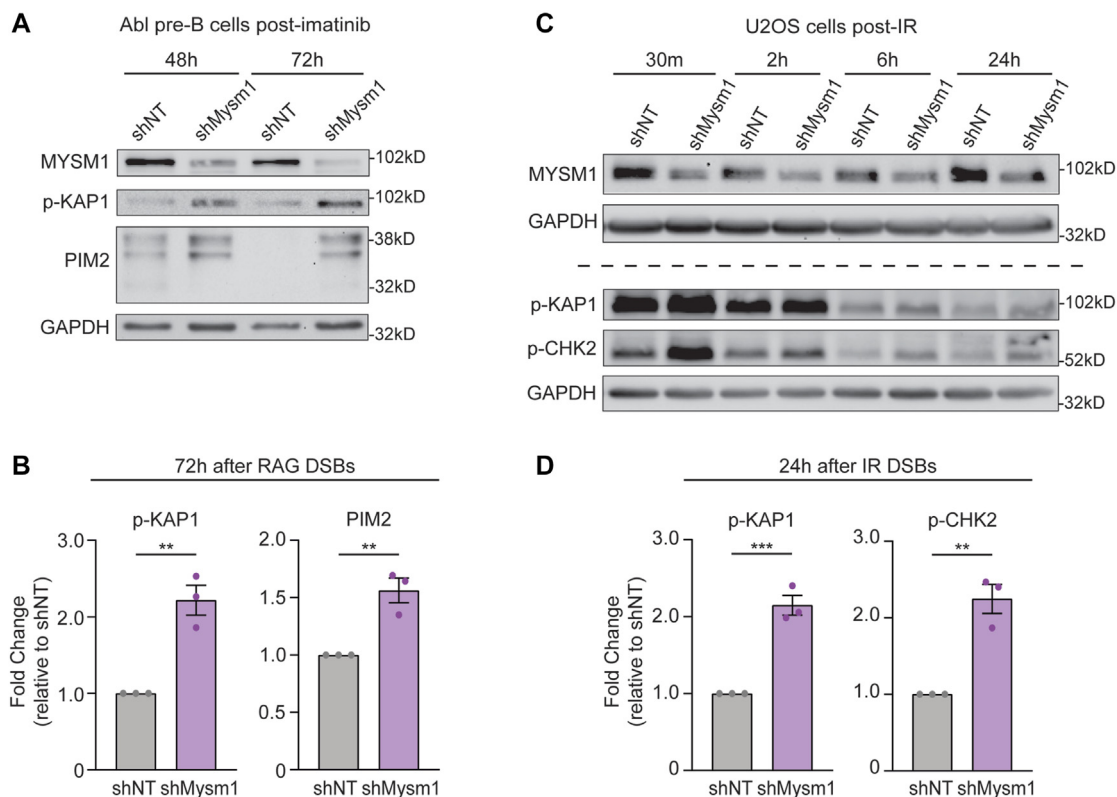
FIG 4. Loss of MYSM1 results in prolonged DDR signaling. **A,** Wild-type abl pre–B cells expressing shNT or shMysm1 (as in Fig 2, A) were treated with imatinib to induce RAG DSBs. Western blot of MYSM1, p-KAP1, and PIM2 at indicated times. GAPDH is loading control. **B,** Quantitation of p-KAP1 and PIM2 at 72 hours in **A**. **C,** U2OS cells expressing shNT or shMysm1 (as in Fig 2, D) were exposed to 10 Gy IR. Western blot analysis of MYSM1, p-KAP1, and p-CHK2 at indicated times. GAPDH is loading control. **D,** Quantitation of p-KAP1 and p-CHK2 at 24 hours in **C**. Data in **A** and **C** are representative of 3 independent experiments. Data in **B** and **D** are mean ± SE from 3 independent experiments. **P < .01; ***P < .001.

B cells (at pre-pro–B-cell stage) results in a marked reduction of pro–B and pre–B cells, the stages where *Ig* recombination occurs.[7,9] MYSM1 was shown to promote expression of *Ebf1, Pax5,* and *Id2,* key transcriptional regulators of B-cell commitment and differentiation.[7,9,18] Expression of EBF1 rescued some abnormalities in MYSM1-deficient B cells *ex vivo*.[9] However, Ebf1-deficient mice have a more severe depletion of early B cells at more primitive developmental stages than observed in Mysm1-deficient mice.[15-17] Additionally, deletion of p53 rescued B-cell development in MYSM1-deficient mice but did not restore the reduced EBF1 expression.[19,59] Thus, while MYSM1-dependent regulation of *Ebf1* may affect B-cell commitment, MYSM1 has additional functions in regulation of B-cell lymphopoiesis.

In addition to altered gene expression, MYSM1-deficient B cells have aberrant DNA damage signals. MYSM1 loss in non–B cells increases sensitivity to DNA damaging agents with increased cell death after ultraviolet or gamma irradiation (our data and others).[2,20] In a multidimensional screen of DUBs, MYSM1 was found to localize to DSBs and to regulate DNA repair and G_2/M checkpoint.[21] We also find that MYSM1 regulates DDR signaling, including phosphorylation of CHK2, a controller of cell cycle checkpoint. In contrast, our studies demonstrate that MYSM1 does not regulate DSB generation or repair. This difference may be secondary to varying degrees of MYSM1 suppression or distinct MYSM1 activities in different

cell types or modes of DNA injury (ie, irradiation vs physiologic DSBs). We find that MYSM1 acts similarly in responses to physiologic RAG-mediated and genotoxic IR-induced DSBs in both B and non–B cells, respectively. However, IR dose, timing of DNA injury relative to cell cycle state, and cell type can all impact DDR. Further investigations are needed to characterize factors that modulate MYSM1 activity in DNA damage.

Loss of MYSM1 results in persistent 53BP1 foci and prolonged DDR signaling in pre–B cells undergoing *Igl* recombination. It is conceivable that, in the absence of MYMS1, RAG DSBs may be repaired by alternative end joining mechanisms, which could trigger distinct DDR kinetics. Using a RAG recombination reporter assay, we find that loss of MYSM1 does not impair GFP expression. In contrast, alternative DSB joining employs end resection, which causes frameshifts or deletions that corrupt the GFP codon. Defects in DNA repair factors (ie, loss of ATM or altered activity of DNA-dependent protein kinase) that disrupt joining or activate alternative end joining invariably result in lower GFP expression.[47,60-62] Thus, our findings support that the changes in DDR signaling with loss of MYSM1 are not a consequence of defects or alterations in RAG DSB repair. Furthermore, while minor variations in sequences of DSB joins may exist, these changes would not be sufficient to trigger the persistent DDR signaling observed in MYSM1 deficiency. Future studies will investigate MYSM1 function in DSB repair pathway selection.
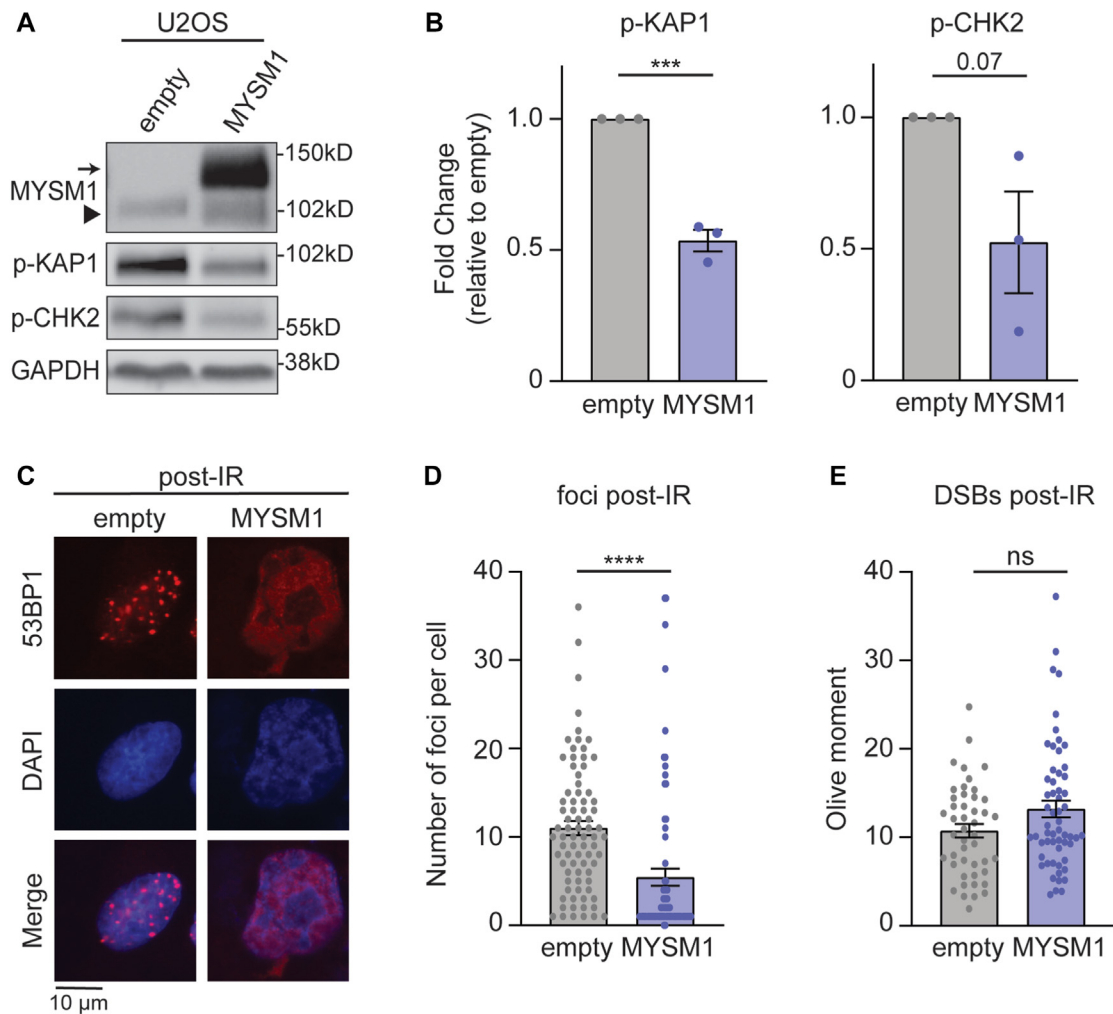
FIG 5. Increased expression of MYSM1 suppresses DDR without altering DSB repair. U2OS cells were transfected with empty vector or vector expressing FLAG-MYSM1 then exposed to 5 Gy IR. Data are at 2 hours after IR. **A,** Western blot of MYSM1, p-KAP1, and p-CHK2. GAPDH is loading control. *Arrow* indicates FLAG-MYSM1. *Arrowhead* indicates endogenous MYSM1. **B,** Quantitation of p-KAP1 and p-CHK2 in **A**. Data are mean ± SE from 3 independent experiments. **C,** Representative images of 53BP1 foci. Bar = 10 μm. **D,** Quantitation of number of foci per cell in **B**. Data are mean ± SEM of 100 cells per condition. **E,** DSBs quantitated by comet assay. Data are mean ± SEM for Olive moment of ≥45 cells per condition. Data in **A, C, D,** and **E** are representative of 3 independent experiments. ***$P < .001$; ****$P < .0001$.

MYSM1 regulates gene expression through deubiquitination of H2AK119Ub.[9,12-14,18] Mice and humans with mutations in *MYSM1* that render it catalytically inactive have a similar phenotype as MYSM1 deficiency, highlighting that MYSM1 affects hematopoiesis and lymphopoiesis through its DUB activity.[3,11] Histone H2A is alternatively ubiquitinated on lysines 13 and 15 (H2AK15Ub) at DSBs by the ubiquitin ligases RNF8 and RNF168.[29-32] 53BP1 binds H2AK15Ub through its ubiquitin-dependent reader motif and subsequently functions as a transducer to coordinate downstream DDR signaling.[33,35] In pre–B cells, 53BP1 prevents DNA end resection to promote joining of RAG DSBs and contributes to transcriptional programming induced by RAG DSBs.[63,64] Following DSB repair, 53BP1 is released from chromatin by DUBs, particularly USP51, which remove K13/15 ubiquitin from H2A.[21,29,30,38,39] We find that loss of MYSM1 leads to prolonged retention of 53BP1 at DSBs and continued DDR signaling, supporting that MYSM1 functions in termination of DDR signaling. Interestingly, while 53BP1 foci

and DDR signals are prolonged in the absence of MYSM1, both continue to decline, suggesting that other DUBs may cooperate with or compensate for MYSM1 to extinguish DDR. The activity of MYSM1 on H2AK15Ub, the role of its DUB activity, and the function of other DUBs in DDR in early B cells are not known. Additionally, it is not evident whether MYSM1 differentiates between H2AK119Ub and H2AK15Ub or acts equally on both sites. MYSM1 is phosphorylated by ATM in response to DNA injury.[26] It is conceivable that this modification alters MYSM1 activity or recruitment to chromatin at DNA damage. These mechanisms of MYSM1 and DDR resolution are currently under investigation.

Patients with MYSM1 deficiency have profound B-cell deficiency that is disproportionate to the reduction in T cells. Testing of patient peripheral blood lymphocytes identified DNA damaging signaling in B cells even in the absence of DNA damaging agents. This result is consistent with our finding that MYSM1 regulates DDR to RAG DSBs in B cells undergoing *Ig* recombination. Our findings also provide mechanistic context for the reduction in

pro– and pre–B cells in MYSM1-deficient mice.[7,9] Heavy chain and light chain *Ig*s are rearranged at these developmental stages and, thus, these stages may be more impacted by DDR dysregulation with MYSM1 loss. T cells also undergo *Ig* recombination (of T-cell receptor loci) and are reduced in MYSM1 deficiency but not to the same magnitude as B cells. Additionally, unlike B cells, T cells do not have evidence of constitutive DDR activation. These differences suggest that MYSM1 may have unique functions in DDR in B cells or, alternatively, that B and T cells have different compensatory mechanisms for managing DDR signaling. It is also conceivable that the profound B-cell lymphopenia in patients with MYSM1 deficiency may result from combined deleterious effects of altered EBF1 expression and abnormal DDRs on developing B cells.

We and others find that MYSM1-deficient B cells have persistence of 53BP1 and γH2AX foci after DNA damage.[2,10,21,59] MYSM1-deficent hematopoietic progenitor cells also have increased γH2AX, which is corrected by deletion of p53 or its downstream effector PUMA (protein product of *BBC3*).[59] Interestingly, the B-cell lymphopenia in *Mysm1*-deficient mice is p53-dependent but PUMA-independent, suggesting that MYSM1 and p53 have unique functions in hematopoietic progenitor cells and B cells. Whether p53 functions in resolution of γH2AX foci in B cells is not known. Our data demonstrate that the persistent γH2AX and 53BP1 foci in *Mysm1*-deficient B cells is secondary to abnormal DDR signaling. Further studies will delineate the contribution of p53 and other DDR pathways to the radiosensitivity and B-cell depletion in patients with MYSM1 variants.

Cumulatively, our findings establish that MYSM1 functions in termination of DDRs to both physiologic and genotoxic DSBs. These studies provide new insights into mechanisms of MYSM1-deficient primary immune deficiency and highlight need for caution in treatment approaches, because patients will be more sensitive to the chemotherapies used for stem cell transplant.

Key messages

- A novel splice variant in MYSM1 results in B-cell lymphopenia, hypogammaglobulinemia, and aberrant responses to DNA damage.
- MYSM1 terminates DDR but does not function in generation or repair of DNA breaks.
- Loss of MYSM1 results in prolonged DNA damage signaling despite normal DNA break repair.

REFERENCES

1. Alsultan A, Shamseldin HE, Osman ME, Aljabri M, Alkuraya FS. MYSM1 is mutated in a family with transient transfusion-dependent anemia, mild thrombocytopenia, and low NK- and B-cell counts. Blood 2013;122:3844-5.
2. Bahrami E, Witzel M, Racek T, Puchalka J, Hollizeck S, Greif-Kohistani N, et al. Myb-like, SWIRM, and MPN domains 1 (MYSM1) deficiency: genotoxic stress-associated bone marrow failure and developmental aberrations. J Allergy Clin Immunol 2017;140:1112-9.
3. Le Guen T, Touzot F, Andre-Schmutz I, Lagresle-Peyrou C, France B, Kermasson L, et al. An in vivo genetic reversion highlights the crucial role of Myb-Like, SWIRM, and MPN domains 1 (MYSM1) in human hematopoiesis and lymphocyte differentiation. J Allergy Clin Immunol 2015;136:1619-26.e5.
4. Li N, Xu Y, Yu T, Yao R, Chen J, Luo C, et al. Further delineation of bone marrow failure syndrome caused by novel compound heterozygous variants of MYSM1. Gene 2020;757:144938.
5. Nanda A, Al-Abboh H, Zahra A, Al-Sabah H, Gupta A, Adekile AD. Neutrophilic panniculitis in a child with MYSM1 deficiency. Pediatr Dermatol 2019; 36:258-9.
6. Forster M, Belle JI, Petrov JC, Ryder EJ, Clare S, Nijnik A. Deubiquitinase MYSM1 is essential for normal fetal liver hematopoiesis and for the maintenance of hematopoietic stem cells in adult bone marrow. Stem Cells Dev 2015;24: 1865-77.
7. Forster M, Farrington K, Petrov JC, Belle JI, Mindt BC, Witalis M, et al. MYSM1-dependent checkpoints in B cell lineage differentiation and B cell-mediated immune response. J Leukoc Biol 2017;101:643-54.
8. Huo Y, Li BY, Lin ZF, Wang W, Jiang XX, Chen X, et al. MYSM1 is essential for maintaining hematopoietic stem cell (HSC) quiescence and survival. Med Sci Monit 2018;24:2541-9.
9. Jiang XX, Nguyen Q, Chou Y, Wang T, Nandakumar V, Yates P, et al. Control of B cell development by the histone H2A deubiquitinase MYSM1. Immunity 2011;35: 883-96.
10. Nijnik A, Clare S, Hale C, Raisen C, McIntyre RE, Yusa K, et al. The critical role of histone H2A-deubiquitinase Mysm1 in hematopoiesis and lymphocyte differentiation. Blood 2012;119:1370-9.
11. Liang Y, Bhatt G, Tung LT, Wang H, Kim JE, Mousa M, et al. Deubiquitinase catalytic activity of MYSM1 is essential in vivo for hematopoiesis and immune cell development. Sci Rep 2023;13:338.
12. Zhu P, Zhou W, Wang J, Puc J, Ohgi KA, Erdjument-Bromage H, et al. A histone H2A deubiquitinase complex coordinating histone acetylation and H1 dissociation in transcriptional regulation. Mol Cell 2007;27:609-21.
13. Vissers JH, Nicassio F, van Lohuizen M, Di Fiore PP, Citterio E. The many faces of ubiquitinated histone H2A: insights from the DUBs. Cell Div 2008;3:8.
14. Wang H, Wang L, Erdjument-Bromage H, Vidal M, Tempst P, Jones RS, et al. Role of histone H2A ubiquitination in Polycomb silencing. Nature 2004;431:873-8.
15. Gyory I, Boller S, Nechanitzky R, Mandel E, Pott S, Liu E, et al. Transcription factor Ebf1 regulates differentiation stage-specific signaling, proliferation, and survival of B cells. Genes Dev 2012;26:668-82.
16. Vilagos B, Hoffmann M, Souabni A, Sun Q, Werner B, Medvedovic J, et al. Essential role of EBF1 in the generation and function of distinct mature B cell types. J Exp Med 2012;209:775-92.
17. Zandi S, Mansson R, Tsapogas P, Zetterblad J, Bryder D, Sigvardsson M. EBF1 is essential for B-lineage priming and establishment of a transcription factor network in common lymphoid progenitors. J Immunol 2008;181:3364-72.
18. Wang T, Nandakumar V, Jiang XX, Jones L, Yang AG, Huang XF, et al. The control of hematopoietic stem cell maintenance, self-renewal, and differentiation by Mysm1-mediated epigenetic regulation. Blood 2013;122:2812-22.
19. Belle JI, Langlais D, Petrov JC, Pardo M, Jones RG, Gros P, et al. p53 mediates loss of hematopoietic stem cell function and lymphopenia in Mysm1 deficiency. Blood 2015;125:2344-8.

20. Kroeger C, Roesler R, Wiese S, Hainzl A, Gatzka MV. Interaction of deubiquitinase 2A-DUB/MYSM1 with DNA repair and replication factors. Int J Mol Sci 2020;21:3762.

21. Nishi R, Wijnhoven P, le Sage C, Tjeertes J, Galanty Y, Forment JV, et al. Systematic characterization of deubiquitylating enzymes for roles in maintaining genome integrity. Nat Cell Biol 2014;16:1016-26.

22. Bednarski JJ, Sleckman BP. At the intersection of DNA damage and immune responses. Nat Rev Immunol 2019;19:231-42.

23. Helmink BA, Sleckman BP. The response to and repair of RAG-mediated DNA double-strand breaks. Annu Rev Immunol 2012;30:175-202.

24. Alt FW, Zhang Y, Meng FL, Guo C, Schwer B. Mechanisms of programmed DNA lesions and genomic instability in the immune system. Cell 2013;152:417-29.

25. Fugmann SD, Lee AI, Shockett PE, Villey IJ, Schatz DG. The RAG proteins and V(D)J recombination: complexes, ends, and transposition. Annu Rev Immunol 2000;18:495-527.

26. Matsuoka S, Ballif BA, Smogorzewska A, McDonald ER 3rd, Hurov KE, Luo J, et al. ATM and ATR substrate analysis reveals extensive protein networks responsive to DNA damage. Science 2007;316:1160-6.

27. Ciccia A, Elledge SJ. The DNA damage response: making it safe to play with knives. Mol Cell 2010;40:179-204.

28. Shiloh Y, Ziv Y. The ATM protein kinase: regulating the cellular response to genotoxic stress, and more. Nat Rev Mol Cell Biol 2013;14:197-210.

29. Uckelmann M, Sixma TK. Histone ubiquitination in the DNA damage response. DNA Repair (Amst) 2017;56:92-101.

30. Aquila L, Atanassov BS. Regulation of histone ubiquitination in response to DNA double strand breaks. Cells 2020;9:1699.

31. Mailand N, Bekker-Jensen S, Faustrup H, Melander F, Bartek J, Lukas C, et al. RNF8 ubiquitylates histones at DNA double-strand breaks and promotes assembly of repair proteins. Cell 2007;131:887-900.

32. Doil C, Mailand N, Bekker-Jensen S, Menard P, Larsen DH, Pepperkok R, et al. RNF168 binds and amplifies ubiquitin conjugates on damaged chromosomes to allow accumulation of repair proteins. Cell 2009;136:435-46.

33. Wilson MD, Benlekbir S, Fradet-Turcotte A, Sherker A, Julien JP, McEwan A, et al. The structural basis of modified nucleosome recognition by 53BP1. Nature 2016;536:100-3.

34. Cuella-Martin R, Oliveira C, Lockstone HE, Snellenberg S, Grolmusova N, Chapman JR. 53BP1 integrates DNA repair and p53-dependent Cell Fate Decisions via Distinct mechanisms. Mol Cell 2016;64:51-64.

35. Fradet-Turcotte A, Canny MD, Escribano-Diaz C, Orthwein A, Leung CC, Huang H, et al. 53BP1 is a reader of the DNA-damage-induced H2A Lys 15 ubiquitin mark. Nature 2013;499:50-4.

36. Shibata A, Jeggo PA. Roles for 53BP1 in the repair of radiation-induced DNA double strand breaks. DNA Repair (Amst) 2020;93:102915.

37. Ward IM, Minn K, Jorda KG, Chen J. Accumulation of checkpoint protein 53BP1 at DNA breaks involves its binding to phosphorylated histone H2AX. J Biol Chem 2003;278:19579-82.

38. Citterio E. Fine-tuning the ubiquitin code at DNA double-strand breaks: deubiquitinating enzymes at work. Front Genet 2015;6:282.

39. Wang Z, Zhang H, Liu J, Cheruiyot A, Lee JH, Ordog T, et al. USP51 deubiquitylates H2AK13,15ub and regulates DNA damage response. Genes Dev 2016;30:946-59.

40. Lancini C, van den Berk PC, Vissers JH, Gargiulo G, Song JY, Hulsman D, et al. Tight regulation of ubiquitin-mediated DNA damage response by USP3 preserves the functional integrity of hematopoietic stem cells. J Exp Med 2014;211:1759-77.

41. Typas D, Luijsterburg MS, Wiegant WW, Diakatou M, Helfricht A, Thijssen PE, et al. The de-ubiquitylating enzymes USP26 and USP37 regulate homologous recombination by counteracting RAP80. Nucleic Acids Res 2015;43:6919-33.

42. Mosbech A, Lukas C, Bekker-Jensen S, Mailand N. The deubiquitylating enzyme USP44 counteracts the DNA double-strand break response mediated by the RNF8 and RNF168 ubiquitin ligases. J Biol Chem 2013;288:16579-87.

43. Matsui M, Kajita S, Tsuchiya Y, Torii W, Tamekuni S, Nishi R. USP49 is a novel deubiquitylating enzyme for gamma H2AX in DNA double-strand break repair. Gene 2022;833:146599.

44. Cousin MA, Smith MJ, Sigafoos AN, Jin JJ, Murphree MI, Boczek NJ, et al. Utility of DNA, RNA, protein, and functional approaches to solve cryptic immunodeficiencies. J Clin Immunol 2018;38:307-19.

45. Bredemeyer AL, Helmink BA, Innes CL, Calderon B, McGinnis LM, Mahowald GK, et al. DNA double-strand breaks activate a multi-functional genetic program in developing lymphocytes. Nature 2008;456:819-23.

46. Soodgupta D, White LS, Yang W, Johnston R, Andrews JM, Kohyama M, et al. RAG-mediated DNA breaks attenuate PU.1 activity in early B cells through activation of a SPIC-BCLAF1 complex. Cell Rep 2019;29:829-843e5.

47. Bredemeyer AL, Sharma GG, Huang CY, Helmink BA, Walker LM, Khor KC, et al. ATM stabilizes DNA double-strand-break complexes during V(D)J recombination. Nature 2006;442:466-70.

48. Johnston R, White LS, Bednarski JJ. Assessing DNA damage responses using B lymphocyte cultures. Methods Mol Biol 2022;2444:69-80.

49. Johnston R, Mathias B, Crowley SJ, Schmidt HA, White LS, Mosammaparast N, et al. Nuclease-independent functions of RAG1 direct distinct DNA damage responses in B cells. EMBO Rep 2023;24:e55429.

50. Bednarski JJ, Nickless A, Bhattacharya D, Amin RH, Schlissel MS, Sleckman BP. RAG-induced DNA double-strand breaks signal through Pim2 to promote pre-B cell survival and limit proliferation. J Exp Med 2012;209:11-7.

51. Bednarski JJ, Pandey R, Schulte E, White LS, Chen BR, Sandoval GJ, et al. RAG-mediated DNA double-strand breaks activate a cell type-specific checkpoint to inhibit pre-B cell receptor signals. J Exp Med 2016;213:209-23.

52. Stewart SA, Dykxhoorn DM, Palliser D, Mizuno H, Yu EY, An DS, et al. Lentivirus-delivered stable gene silencing by RNAi in primary cells. RNA 2003;9:493-501.

53. Zhao Y, Mudge MC, Soll JM, Rodrigues RB, Byrum AK, Schwarzkopf EA, et al. OTUD4 is a phospho-activated K63 deubiquitinase that regulates MyD88-dependent signaling. Mol Cell 2018;69:505-516e5.

54. Lek M, Karczewski KJ, Minikel EV, Samocha KE, Banks E, Fennell T, et al. Analysis of protein-coding genetic variation in 60,706 humans. Nature 2016;536:285-91.

55. Richards S, Aziz N, Bale S, Bick D, Das S, Gastier-Foster J, et al. Standards and guidelines for the interpretation of sequence variants: a joint consensus recommendation of the American College of Medical Genetics and Genomics and the Association for Molecular Pathology. Genet Med 2015;17:405-24.

56. Teng G, Maman Y, Resch W, Kim M, Yamane A, Qian J, et al. RAG represents a widespread threat to the lymphocyte genome. Cell 2015;162:751-65.

57. Tirosh I, Yamazaki Y, Frugoni F, Ververs FA, Allenspach EJ, Zhang Y, et al. Recombination activity of human recombination-activating gene 2 (RAG2) mutations and correlation with clinical phenotype. J Allergy Clin Immunol 2019;143:726-35.

58. Tubbs AT, Dorsett Y, Chan E, Helmink B, Lee BS, Hung P, et al. KAP-1 promotes resection of broken DNA ends not protected by gamma-H2AX and 53BP1 in G(1)-phase lymphocytes. Mol Cell Biol 2014;34:2811-21.

59. Belle JI, Petrov JC, Langlais D, Robert F, Cencic R, Shen S, et al. Repression of p53-target gene Bbc3/PUMA by MYSM1 is essential for the survival of hematopoietic multipotent progenitors and contributes to stem cell maintenance. Cell Death Differ 2016;23:759-75.

60. Zhu Y, Jiang W, Lee BJ, Li A, Gershik S, Zha S. Phosphorylation of DNA-PKcs at the S2056 cluster ensures efficient and productive lymphocyte development in XLF-deficient mice. Proc Natl Acad Sci U S A 2023;120:e2221894120.

61. Zha S, Guo C, Boboila C, Oksenych V, Cheng HL, Zhang Y, et al. ATM damage response and XLF repair factor are functionally redundant in joining DNA breaks. Nature 2011;469:250-4.

62. Bredemeyer AL, Edwards BS, Haynes MK, Morales AJ, Wang Y, Ursu O, et al. High-throughput screening approach for identifying compounds that inhibit nonhomologous end joining. SLAS Discov 2018;23:624-33.

63. Innes CL, Hesse JE, Morales AJ, Helmink BA, Schurman SH, Sleckman BP, et al. DNA damage responses in murine Pre-B cells with genetic deficiencies in damage response genes. Cell Cycle 2020;19:67-83.

64. Difilippantonio S, Gapud E, Wong N, Huang CY, Mahowald G, Chen HT, et al. 53BP1 facilitates long-range DNA end-joining during V(D)J recombination. Nature 2008;456:529-33.

PATIENT CLINICAL SUMMARY

Initial presentation

A 1-week-old healthy, Black male presented with abnormal newborn screen for severe combined immune deficiency with a cycle threshold value of 45 (reference <36) on real-time PCR for T-cell receptor excision circles. Patient was born by spontaneous vaginal delivery to an 18-year-old mother at estimated gestational age of 37 weeks. Maternal pregnancy was complicated by type I diabetes, treated gonococcal infection, and intrauterine growth retardation. Postnatal course was complicated by low birth weight of 2140 g and persistent hypoglycemia. Testing for congenital cytomegalovirus infection was negative. He was discharged on day 4 of life in good health and had no intercurrent infections or illnesses. Family history was notable for neurofibromatosis type 2 in paternal aunt but was negative for immunodeficiency, infant death, or consanguinity. He has a 2-year-old paternal half-brother who is healthy.

Physical examination revealed an afebrile, small infant with weight 2125 g, length 41 cm, and head circumference 30 cm, all below the third percentile for age. No craniofacial dysmorphic features or deformities of extremities were noted. Cardiac exam was without murmur and lungs were clear. He had an exaggerated tonic neck reflex bilaterally and mild hypertonicity of extremities. Remainder of neurological exam was normal.

Brain magnetic resonance imaging, obtained due to the increased muscle tone, demonstrated nonspecific, scattered T_1 hyperintensities within the globus pallidus bilaterally. Ophthalmology exam showed large magnitude infantile exotropia. Hearing test by auditory brain stem response was normal. Bone survey revealed normal bone mineralization with slightly delayed bone age and no deformities. Echocardiogram showed normal systolic function and normal anatomy with mild dilatation of left atrium and ventricle.

Laboratory evaluation on admission (day of life 8) showed white blood cell count of 7,000 cells/mL, hemoglobin of 13.9 g/dL, and platelets of 636,000/mL. Absolute lymphocyte count was 1,500 cells/mL and absolute neutrophil count was 4,800 cells/mL. Flow cytometric evaluation of immune cell populations identified nearly absent B cells, low T cells, and normal NK-cell numbers (Fig 1, *A*). Of the total CD4$^+$ T cells, 60% expressed CD45RA (Fig 1, *A*). Naïve CD31$^+$CD45RA$^+$CD4$^+$ T cells were slightly reduced at 30% (normal >64%-95%). Repeat T-cell receptor excision circles testing was low at 1,010 copies per 10^6 CD3$^+$ cells (normal >6,794). T-cell proliferation to phytohemagglutinin was normal (>90%). No maternal T-cell engraftment was present. IgM and IgA were low but IgG was normal (Fig 1, *A*). HIV DNA PCR was negative. Testing of adenosine deaminase and purine nucleoside phosphorylase enzyme activity were normal. Telomere length testing was normal (75th percentile).

Genetic testing

Clinical NextGen sequencing and concurrent deletion/duplication testing of a panel of 26 genes associated with severe combined immune deficiency (*ADA, AK2, ATM, CD3D, CD3E, CD3Z, CORO1A, DCLRE1C, DOCK8, FOXN1, IL2RG, IL7R, JAK3, LIG4, NHEJ1, ORAI1, PNP, PRKDC, PTPRC, RAC2, RAG1, RAG2, RMRP, STIM1, TBX1,* and *ZAP70*) was negative. Chromosome microarray revealed paternal uniparental disomy of the entirety of chromosome 1. Subsequent clinical whole exome sequencing on patient and both parents identified a paternal homozygous variant in *MYSM1* (c.1843-1G>A, IVS15-1 G>A variant) due to uniparental disomy. This variant is a mutation in a splice acceptor site and is predicted to result in aberrantly spliced mRNA. The variant is not observed in a large population.[E1]

Clinical course

The patient was started on monthly intravenous immunoglobulin and prophylactic acyclovir and fluconazole. Prophylactic trimethoprim/sulfamethoxazole was initiated at 4 weeks of age. At 6 weeks of age, he developed normocytic anemia (hemoglobin 6.4 g/dL) with inappropriately low reticulocytosis (3%). Direct and indirect Coombs were negative. Glucose-6-phosphate dehydrogenase level was normal. Bone marrow biopsy revealed multilineage hematopoiesis. He required monthly blood transfusions. Trimethoprim/sulfamethoxazole was changed to monthly pentamidine due to a concern of possible bone marrow suppression. Over the subsequent 2 months, T and B cells remained very low (Fig 1, *A*), and he had 3 episodes of fever without identified sources. T-cell proliferation to phytohemagglutinin was repeated at 2 weeks and 4 months of age and remained normal.

Hematopoietic stem cell transplant

Due to the persistent T-cell lymphopenia and transfusion-dependent anemia, the patient was evaluated for hematopoietic stem cell transplant. Patients with MYSM1 deficiency have been successfully transplanted with resultant reconstitution of normal bone marrow and immune function.[E2] Our patient proceeded to hematopoietic stem cell transplant at 5 months of age. In light of the radiosensitivity results, a reduced intensity conditioning regimen with low-dose busulfan (target AUC of 40-60 mg × h/L divided over 4 days administered every 6 hours from days −5 to −2), fludarabine (30 mg/m^2/d on days −8 to −3) and antithymocyte globin (30 mg/kg/d on days −5 to −2) was used followed by infusion of mismatch (5 of 6) cord blood product. Graft-versus-host disease prophylaxis included mycophenolate mofetil and tacrolimus.

He tolerated conditioning therapy well. On day 5 post-transplant (after infusion of stem cells), he developed fevers with neutropenia (absolute neutrophil count 400 cells/mL). He was empirically treated with cefepime and vancomycin. Due to persistence of fevers, amphotericin B was added. Blood cultures had no growth. Testing for EBV, cytomegalovirus, human herpesvirus 6, adenovirus was negative. On day 9 post-transplant, he developed elevated liver enzymes (aspartate transferase 374, alanine transaminase 532, alkaline phosphatase 197, and lactate dehydrogenase 999 units/L), hyperferritinemia (63,622 ng/mL; normal 50-200), ascites, and fluid retention. Abdominal ultrasound showed normal liver without biliary ductal dilatation. Due to concern for veno-occlusive disease, defibrotide was started with resultant decrease in liver enzymes. However, he rapidly progressed to acute renal failure with peak creatinine of 1.32 mg/dL (reference 0.1-0.6). On day 13 post-transplant, he was transferred to intensive care unit for hypoxemia requiring intubation and hypertension treated with amlodipine. Chest

x-ray demonstrated pulmonary edema. He was initiated on continuous renal replacement therapy. He subsequently was noted to have eye deviation and abnormal limb movement. Electroencephalogram showed diffuse encephalopathy without epileptiform features. Head computed tomography showed no acute intracranial abnormalities. Lumbar puncture was deferred due to unstable conditions. Despite stabilized blood pressure, ventilatory support, and correction of electrolytes imbalance, he became profoundly bradycardic and progressed to pulseless electrical activity. Cardiopulmonary resuscitation was initiated but was unsuccessful, and the patient died on day 14 post-transplant. A postmortem evaluation was declined by the family and not performed.

REFERENCES

E1. Lek M, Karczewski KJ, Minikel EV, Samocha KE, Banks E, Fennell T, et al. Analysis of protein-coding genetic variation in 60,706 humans.. Nature 2016; 536:285-91.

E2. Bahrami E, Witzel M, Racek T, Puchalka J, Hollizeck S, Greif-Kohistani N, et al. Myb-like, SWIRM, and MPN domains 1 (MYSM1) deficiency: genotoxic stress-associated bone marrow failure and developmental aberrations.. J Allergy Clin Immunol 2017;140:1112-9.

A

	Exon 15	Exon 16	Exon 17	Exon 18
MYSM1 REF	ATACTCAGAAGTTGATAAAGTAGTTGAA	GTCTGT...TACCAG	AGTTAC...TCTTATC	GCTTAC
HC (bottom)	GAAGTTGATAAAGTAGTTGAA	GTCTGT...TACCAG	AGTTAC...TCTTATC	GCTTAC
PT	CTCAGAAGTTGATAAAGTAGTTGAA		AGTTAC...TCTTATC	GCTTAC

B

	Exon 15	Exon 16	Exon 17	alternate splice	Exon 18
MYSM1 X4	ACTCAGAAGTTGATAAAGTAGTTGAA	GTCTGT...TACCAG	AGTTAC...TCTTATC	AAATCCTCT...TAACTCAG	GCTTAC
HC (top)	CAGAAGTTGATAAAGTAGTTGAA	GTCTGT...TACCAG	AGTTAC...TCTTATC	AAATCCTCT...TAACTCAG	GCTTAC
MYSM1 REF	ATACTCAGAAGTTGATAAAGTAGTTGAA	GTCTGT...TACCAG	AGTTAC...TCTTATC		GCTTAC
HC (bottom)	GAAGTTGATAAAGTAGTTGAA	GTCTGT...TACCAG	AGTTAC...TCTTATC		GCTTAC
PT	CTCAGAAGTTGATAAAGTAGTTGAA		AGTTAC...TCTTATC		GCTTAC

FIG E1. Abnormal mRNA splicing due to novel MYSM1 variant. RT-PCR products in Fig 1, *B* for exons 15-18 of mRNA from PMBCs of PT and HC were sequenced and aligned to **(A)** *MYSM1* mRNA reference sequence (NM_001085487.3, REF) and to **(B)** *MYSM1* mRNA isoform X4 (XR_946533, X4). HC (*top*) indicates higher molecular weight band and HC (*bottom*) indicates lower molecular weight band. Exons are labeled above the sequences.
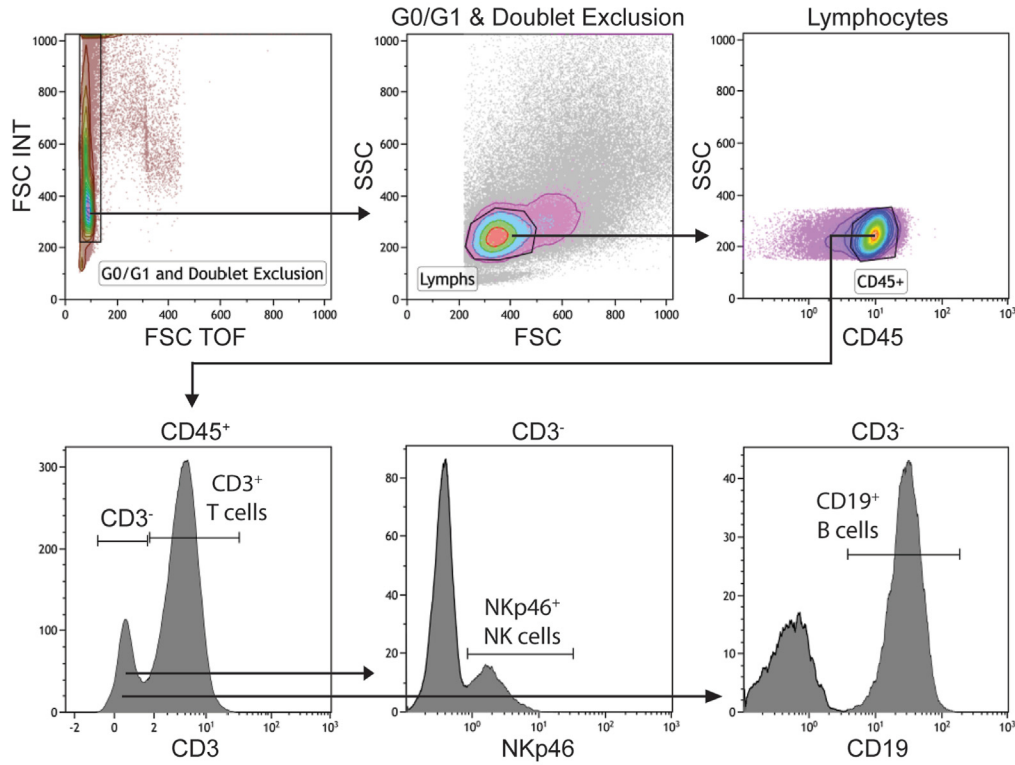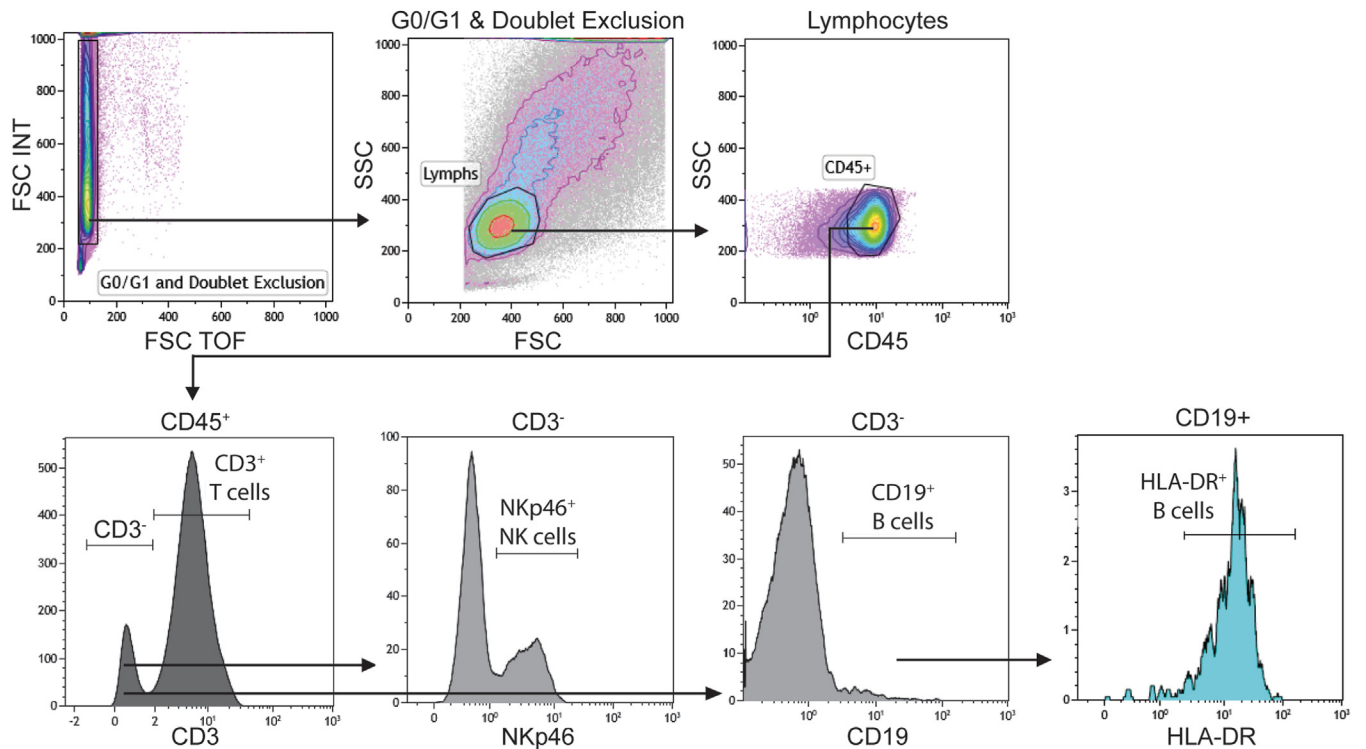
A Healthy Control (HC) PBMCs

B Patient (PT) PBMCs

FIG E2. Gating strategy for assessment of DNA damage signals in peripheral blood lymphocytes. PMBCs were stained with anti-CD45, anti-CD3, anti-CD19, and anti-NKp46. Gating approach to identify T cells, B cells, and NK cells for DNA damage signaling assessments in Fig 1, F and Fig E3 is shown for HC **(A)** and PT **(B)**. T cells: $CD45^+CD3^+$. NK cells: $CD45^+CD3^-NKp46^+$. B cells: $CD45^+CD3^-CD19^+$. PBMCs from PT were also stained with anti-HLADR to confirm B-cell identity ($CD45^+CD3^-CD19^+HLADR^+$). *FSC*, forward scatter; *INT*, intensity; *SSC*, side scatter; *TOF*, time of flight.
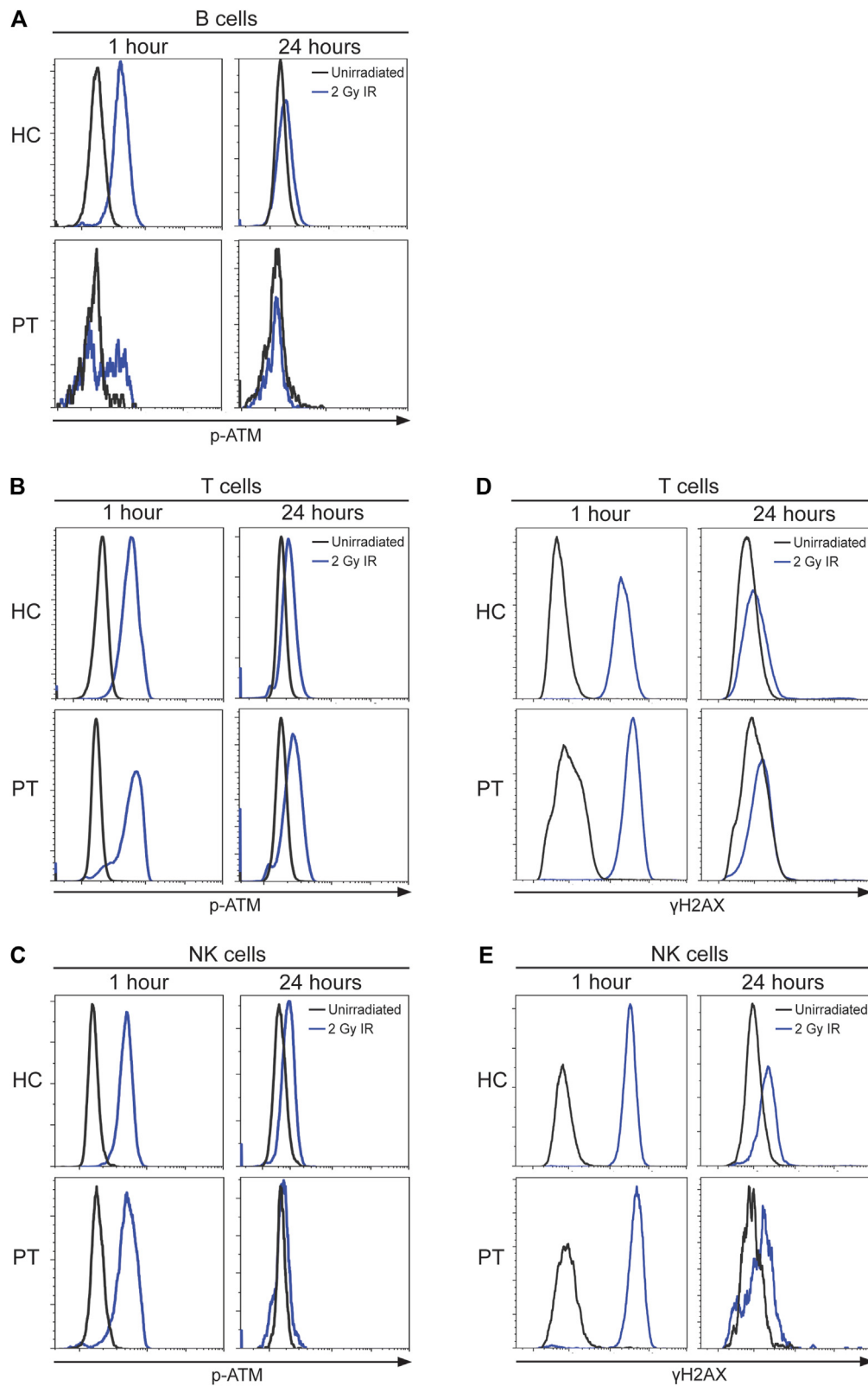
FIG E3. DNA damage signaling in lymphocytes of patient with novel MYSM1 splice variant. Flow cytometry of p-ATM in B cells **(A),** T cells **(B),** and NK cells **(C)** from HC and PT at indicated times after 2 Gy IR (*blue lines*). Unirradiated cells (*black lines*) included at each time as control. Flow cytometry of γH2AX in T cells **(D)** and NK cells **(E)** from HC and PT at indicated times after 2 Gy IR (*blue lines*). Unirradiated cells (*black lines*) included at each time as control.
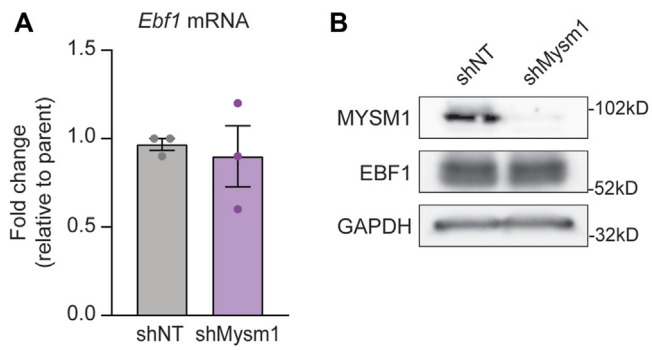
FIG E4. Suppression of MYSM1 in pre–B cells does not alter EBF1 expression. Wild-type abl pre–B cells were transduced with retrovirus expressing shNT or shMysm1. **A,** RT-PCR of *Ebf1* mRNA. Data are mean ± SE from 3 independent experiments. **B,** Western blot of EBF1 and MYSM1. GAPDH is loading control. Data are representative of 3 independent experiments.

TABLE E1. Primers used for PCR over the break and RT-PCR

Primer name	Species	Application	Sequence
MYSM1_(exon 1-6)_FWD	Human	RT-PCR	ATGTGGATATCGAAGGGGACG
MYSM1_(exon 1-6)_REV	Human	RT-PCR	AGCTCTTTTTCTTCTATCGTCCAC
MYSM1_(exon 12-16)_FWD	Human	RT-PCR	AAGAGAAGAGGAAAAAGGCAGACC
MYSM1_(exon 12-16)_REV	Human	RT-PCR	GATCCATCTCACACTGTAGTCCTG
MYSM1_(exon 15-18)_FWD	Human	RT-PCR	AGGAGGAAGATACTCAGAAGTTGA
MYSM1_(exon 15-18)_REV	Human	RT-PCR	TAATCCCCACTGAGGTTCTTCTAA
MYSM1_FWD	Human	RT-PCR	GGACAAAGGCATGGACACCATC
MYSM1_REV	Human	RT-PCR	TTGAAGACAGCCCTTGGAAGAC
B-actin_F	Human/mouse	RT-PCR	TCATCACTATTGGCAACGAGCGGTTC
B-actin_R	Human/mouse	RT-PCR	TACCACCAGACAGCACTGTGTTGGCA
EBF1_FWD	Mouse	RT-PCR	CCCACAACAACCAGGAGATTAT
EBF1_REV	Mouse	RT-PCR	TGCATGGACCGAAGTGTTAG
Jk1_FWD	Mouse	qPCR for DSBs	GCTACCCACTGCTCTGTTCC
Jk1_REV	Mouse	qPCR for DSBs	CCTTGGAGAGTGCCAGAATC
CD19_FOR	Mouse	qPCR for DSBs	TGTCTCCTTCCTCCTCTTTCT
CD19_REV	Mouse	qPCR for DSBs	CTCAACTCAGAACCCAGACTTT

qPCR, Quantitative PCR.